Fused Deposition Modeling of Metals

Jorge Mireles[1], David Espalin[1], David Roberson[1], Bob Zinniel[2], Francisco Medina[1], Ryan Wicker[1]

1. W.M. Keck Center for 3D Innovation, The University of Texas at El Paso, El Paso, TX
2. Stratasys, Inc., Eden Prairie, MN

REVIEWED, Accepted August 22, 2012

Abstract

Studies have been conducted to improve previous work performed in developing a Fused Deposition Modeling for metals (FDMm) system used for applications in electronics and fabrication of 3-dimensional metallic structures. A FDM 3000 system was modified to achieve controlled deposition of eutectic Bi58Sn42 and non-eutectic Sn60Bi40 materials. Toolpath command modifications were required to achieve controlled deposition of metals. Results are presented which include a redesigned metal deposition head, computer modeling of fluid flow, and finally examples of the successful deposition of metal alloys. Additionally, FDMm-fabricated metal samples were prepared and analyzed using optical and scanning electron microscopy. Controlled deposition of metals using FDMm allows for parts that can be used for jigs and fixtures, electroforming mandrels, encapsulation molds, dies, electronic joining applications, as well as printing 3-dimensional electronic circuitry.

1 Introduction

Additive manufacturing (AM) allows complex parts to be built without the need for tooling, dies, or molds, using little human intervention. Fused Deposition Modeling (FDM) technology is an AM process that builds 3D shapes by taking filaments of thermoplastic polymer materials and driving them into a heated liquefier to be extruded through a small diameter nozzle onto a build platform. Technologies capable of processing metals include, for example, electron beam melting, direct metal laser sintering, laser engineered net shaping and selective laser melting. Utilizing FDM technology to extrude metals poses advantages and disadvantages when compared to methods that currently build using metal alloys. An advantage of using FDM is the lack of expensive lasers equipped in sintering processes or an electron beam as is present in the electron beam melting process. Less expensive materials and systems are available that use FDM technology compared to sintering and melting technologies. A difference is also the ability to build using both thermoplastics and metals within the same build which is not possible with other direct metal systems. Disadvantages include the limitation to low-temperature, low-strength, alloys as well as the possibility for oxidation during the build process due to the lack of a controlled environment. Extending FDM to be able to process metal alloys, called FDM for metals (FDMm), has been the subject of previous work where successful deposition of tin-bismuth (Sn60Bi40 and Bi58Sn42) alloys was demonstrated (Mireles *et al.*, 2012) . Prior research in metallic FDM with metal/polymer filaments showed successful fabrication of 3D structures (Masood and Song, 2004; Agarwala *et al*., 1996); however, the parts were shown to possess insufficient material properties, such as conductivity, as compared to the bulk or pure alloys (i.e. metals without a polymer binder). The research presented here utilizes a Stratasys FDM 3000 system to deposit low melting temperature (T_m) alloys (i.e. alloys of T_m below ~300^{o}C), similar to the system described in Mireles *et al*., 2012. Drawbacks in the system described in Mireles *et al.*, 2012, include a liquefier design which presents unnecessary frictional effects due to a 90^o bend and liquefier length which poses start/stop deposition issues with the

molten droplets as has been prevalent in microdispensing techniques (Bellini and Bertoldi, 2004; Bellini, 2002).

The work presented here extends the concepts described in Mireles *et al.*, 2012 to more effectively deposit low T_m metal alloys using a redesigned deposition head. The redesigned liquefier was conceived using current liquefier designs of machines currently produced by Stratasys (FDM Titan, FDM Maxum, 400mc, 900mc) as well as 3D printers which use the concepts of FDM and use straight liquefier configurations (MakerBot, 3DTouch). Previous work by Rice *et al*. 2000 has attempted to deposit low T_m metals using a modified design that implements a rheocast liquefier that uses the basic FDM process of layer-to-layer stacking with metal slurries of binary alloys instead of a wire feed process. However, the layer thickness produced using the rheocast liquefier system only achieves layer thickness on the order of 3.5mm (0.135in). Modifications of temperature, flow parameters, as well as toolpath commands have been modified to achieve controlled deposition. Flow modeling of both the redesigned and the original liquefier design are discussed with experimental results as well as possible ways to implement such designs with high temperature alloys. Metallographic images have been taken to observe the microstructure of parts built using FDMm and determine possible implications or advantages of using a FDMm system to build both electronic circuitry and 3D parts. The applications that can benefit from low T_m metal alloys include building jigs and fixtures, electroforming mandrels, encapsulation molds, dies, electronic joining applications, as well as printing 3-Dimensional circuitry (Ojebuoboh, 1992; White and Ferriter, 1990). The following describes the design and development of the redesigned FDMm liquefier, fluid flow modeling comparing original and redesigned liquefiers, followed by deposition results, and a successful example of the fabrication of a 3D object.

2 Design and concept

A FDM 3000 system (Stratasys, Inc., Eden Prairie, MN) was used in this research due to its ability to alter build parameters such as deposition head motion speed, material flow rates, chamber and liquefier temperatures, and toolpath commands. Modern FDM systems, such as the Fortus 900mc and 400mc, include a straight liquefier configuration that formed the basis for a redesign of the FDM 3000 head. Figure 1(a) shows the original configuration for a FDM 3000 deposition head and Figure 1(b) shows the redesigned liquefier implemented in this research.

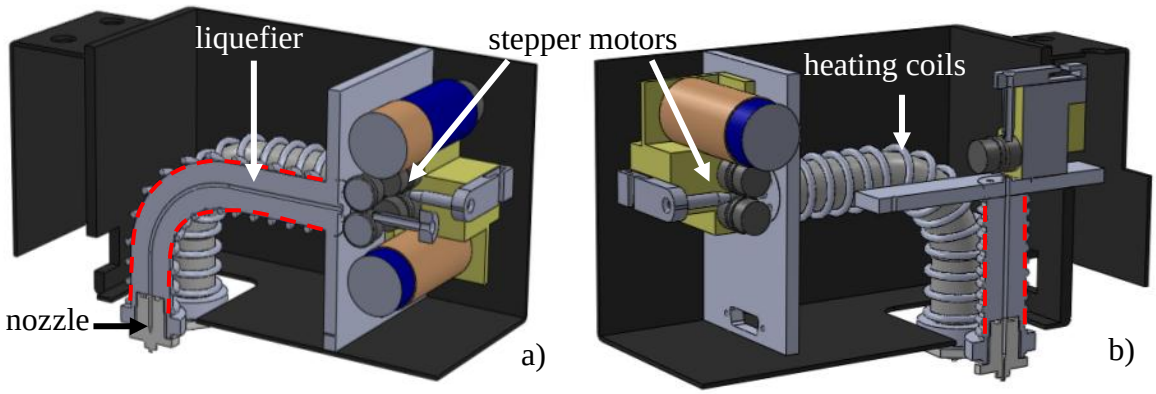

Figure 1: FDM head of a) original liquefier design and b) redesigned liquefier showing difference in liquefier configuration (note that the original liquefiers is curved while the redesigned liquefier is straight as highlighted by red dashed lines)

The redesigned liquefier was meant to remove the 90^o bend to enable the reduction of drive forces required to deliver material as well as facilitate the reduction of puddling effects due to extra material being dispensed after the stepper motors are commanded to stop – a problem inherent to the original liquefier design. Also, the liquefier was shortened to 1) improve transient response due to the starting and stopping of the stepper motors to achieve uniform line thicknesses, 2) reduce pressure to minimize driving forces that can sometimes lead to buckling and puddling, and 3) improve heat transfer through a more concentrated heat coil configuration to achieve a smaller temperature gradient between the liquefier inlet and outlet. Through the use of a redesigned liquefier, it was hypothesized that material deposition would be better controlled in start/stop operations (i.e. material will not spill or puddle), friction effects will be reduced by incorporating a straight liquefier, and better heat transfer from the liquefier inlet to the nozzle exit.

3 Experiments and methods

3.1 Modeling

Modeling of flow was performed with the use of ADINA software (ADINA R&D, Inc., Watertown, MA) to qualitatively demonstrate the benefits of the redesigned liquefier. The 2D geometries were replicated for the redesigned and original liquefier versions and the same boundary conditions were applied in the modeling. The boundary conditions were laminar flow, no-slip conditions between the liquefier walls and the molten metal alloy, fluid incompressibility, gravitational acceleration of $9.8 m/s^2$ acting on the fluid, steady-state conditions, (Roxas and Ju, 2008, Bellini, 2002), inlet velocity of 3.73mm/s (0.147in/s) (as measured), and the material properties for molten Sn-Bi alloy of 15,000cP (as measured for molten alloy using a Brookfield DV-E Viscometer).

3.2 Experiments and methods

Experimentation performed on the fluid flow was qualitative, as instrumentation to measure pressure was unavailable, and results included observations of material flow through each nozzle. To build complex 2D shapes as well as facilitate the stacking of layers, modifiable toolpath commands were generated using Insight software (Stratasys Inc., Eden Prairie, MN) from a corresponding CAD file. A modified tip was also used which has an increased nozzle diameter of 0.635mm (0.025in) that allows for improved deposition of molten metal and decreases pressure within the liquefier allowing the filament to be fed with less applied force by the servo motors. During the build process, the layer thickness (deposition head movement in Z-direction) was modified to account for increased deposition from the modified tip to achieve a layer thickness of 0.762mm (0.03in). Other build parameters changed include the slowdown of the deposition head velocity, the flow, and the liquefier temperature. The deposition head velocity was decreased to 750microsteps per second from 1000microsteps per second. A full explanation of the flow parameter modification is found elsewhere (Mireles *et al*., 2012).

Additionally, experiments involving the variation of thermal attributes were performed using type K thermocouples. The liquefier temperature was set to 220^oC through the temperature controllers in the FDM 3000. The envelope temperature was set to ambient temperature and the neighboring liquefier was set to a lower temperature (210^oC) and the tip was removed to avoid excess heat transfer between the model and support liquefiers. A thermocouple was placed at the nozzle tip and the temperature was read once the system reached

steady temperature conditions. The liquefier temperature was set to 210°C for the eutectic alloy Bi58Sn42 and 220°C for the non-eutectic alloy Sn60Bi40. These temperatures account for a temperature difference from the heat supplied to the liquefier by the heating coils to the heat conducted to the nozzle end.

Scanning electron microscopy (SEM) was performed with a Hitachi S-4800 Ultra-high Resolution Field Emission Scanning Electron Microscope (Hitachi High-Technologies Corporation, Tokyo, Japan) equipped with an EDAX energy dispersive X-ray analyzer (EDS) and utilizing a 20keV accelerating voltage. Optical metallography was performed using a Leica MEF4M optical digital imaging system on a mounted sample of stacked layers built using the FDMm system. Metallography was performed on the mounted samples using 400grit, 1000grit, and 1200grit paper, followed by a finishing step with a polishing cloth using 0.3µ alumina slurry. An etchant composed of 10% HCl and 90%H_2O was applied to reveal the microstructure.

4 Results

4.1 Modeling results

Figure 2 shows the flow modeling and pressure results for the original liquefier design (Figure 2(a)) and the redesigned liquefier (Figure 2(b)). Pressure was of importance since it directly affects how the material is manipulated during deposition (i.e. a greater pressure drop increases the amount of force needed to push the material filament to achieve extrusion) (Bellini, 2002; Roxas and Ju, 2008). The pressure drop between both designs differed and was ~14% greater in the original liquefier design. The same modeling methodology was also performed in different research where a curve liquefier was modeled (Ramanath *et al.*, 2008); separate work modeled a straight liquefier (Bellini, 2002) and both showed noteworthy differences between designs. During metal deposition experiments, the start and stop behavior of flow was observed and showed continued flow after the filament was no longer fed using the original liquefier. The continued flow was not observed when using the redesigned liquefier and may be due to the difference in liquefier length and the liquidus properties of the metal alloy inside the liquefier. The amount of force needed to push the filament to facilitate continuous deposition was also reduced 150% from previous research results (Mireles *et al.*, 2012) which was likely attributed to

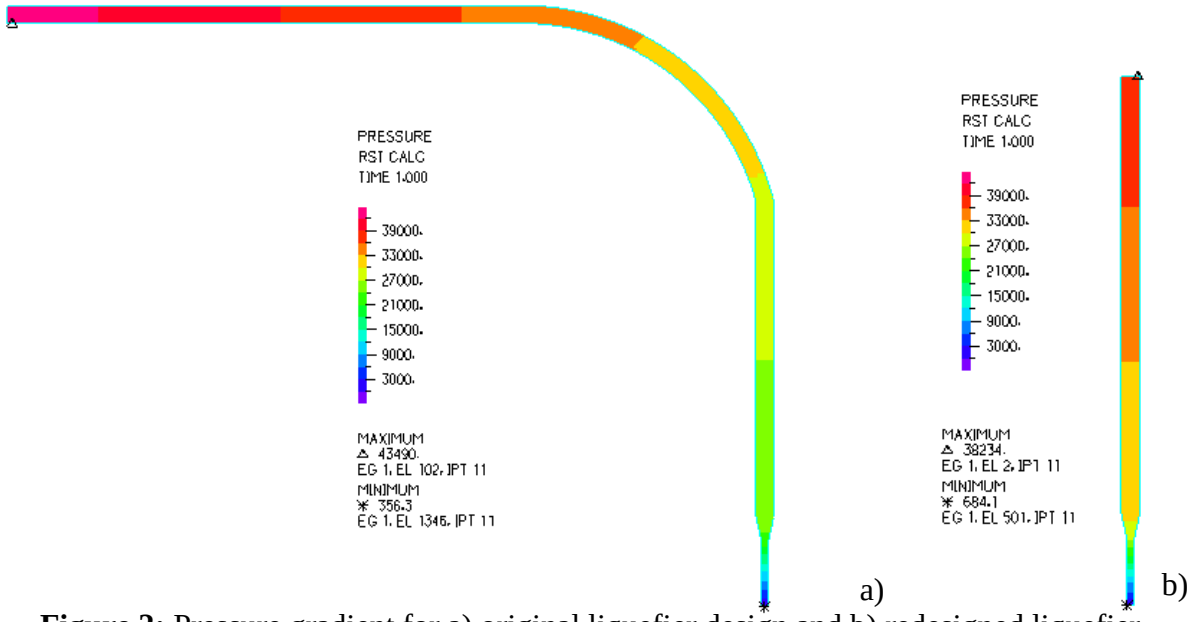

Figure 2: Pressure gradient for a) original liquefier design and b) redesigned liquefier

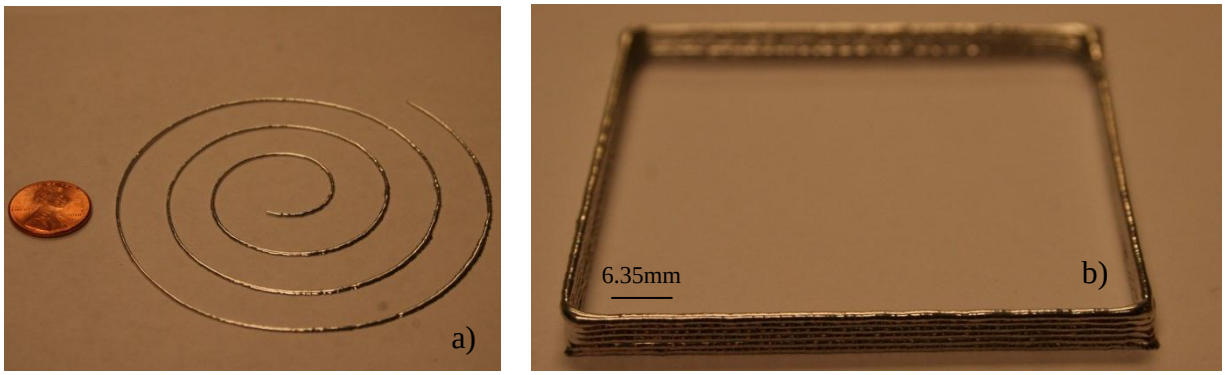

Figure 3: Demonstration of deposition results using FDMm where a) shows an example of 2D shapes and b) shows a 3D structure of 6 stacked layers.

lowering the pressure with the redesigned liquefier. Additionally, experimentation performed utilizing type K thermocouples showed a difference between the temperature set by the operator (220°C) to the temperature at the nozzle of 65°C for the original liquefier design compared to 48°C for the redesigned liquefier demonstrating improved precision.

Using ideal conditions, the simulation results for pressure still showed a notable difference between both designs. The non-ideal conditions including frictional effects, slip between the liquefier walls and the filament, as well as uneven heat distribution, can produce a greater difference between the two liquefier designs and demonstrates the need for a straight liquefier design as this design minimizes the non-ideal conditions. Further emphasizing the need for a straight liquefier design is the fact that similar designs are already used in newer FDM models.

4.2 Deposition results

To demonstrate the improved capability of the redesigned liquefier as well as the effect of code modifications and liquefier temperature changes, 2D and 3D structures were fabricated and are shown in Figure 3(a) and Figure 3(b), respectively. As shown, layer stacking was achieved and parts were created using metal alloys of low T_m. Road width of the layers using eutectic material was 1.24mm (0.049in) and layer thickness was 0.74mm (0.029in). For non-eutectic material, road width was 1.12mm (0.44in) and layer thickness was 0.71mm (0.028in). As

Table 1: Comparison of 10 single layers each of Sn-Bi or ABS

	Bi58Sn42	Sn60Bi40	ABS
Z Thickness, μ± σ (mm (inch))	0.74± 0.13 (0.029±0.0051)**	0.71±0.061 (0.028±0.0024)**	0.254 (0.010)*
Road Width, μ± σ (mm (inch))	1.24±0.19 (0.049±0.0078)**	1.12±0.12 (0.044±0.0045)**	0.76 (0.030)*
System Temperature (°C)	210°C(428°F)**	220°C(446°F)**	270°C(518°F)*
Tensile Strength (MPa)	51.7***	52.5***	22***
Elongation at Break (%)	35***	35***	6***
***According to system specifications, standard deviation not available**			
****According to deposition results**			
***** According to manufacturer information**			

demonstrated in previous research(Mireles *et al.*, 2012), non-eutectic materials deposited better than eutectic materials and it was also demonstrated here by observing the standard deviation between single lines of deposited material in Table 1.

Results of the deposition of low T_m metallic materials also extend to the continuity and thickness uniformity throughout the deposited lines. As shown in Figure 3, the lines for both 2D and 3D parts are continuous throughout. It was previously hypothesized that non-eutectic materials are more suitable for FDM due to the presence of a "mushy" zone which allows for a higher viscosity and therefore deposition was more controlled and continuous (Mireles *et al.*, 2012, White and Ferriter, 1990). The results in Table 1 showed little difference between both eutectic and non-eutectic materials, however, non-eutectic lines still showed less variance in thickness throughout the length of a deposited line. Although non-eutectic alloys still perform better than eutectic compositions, the redesigned liquefier improves the deposition of eutectic alloys.

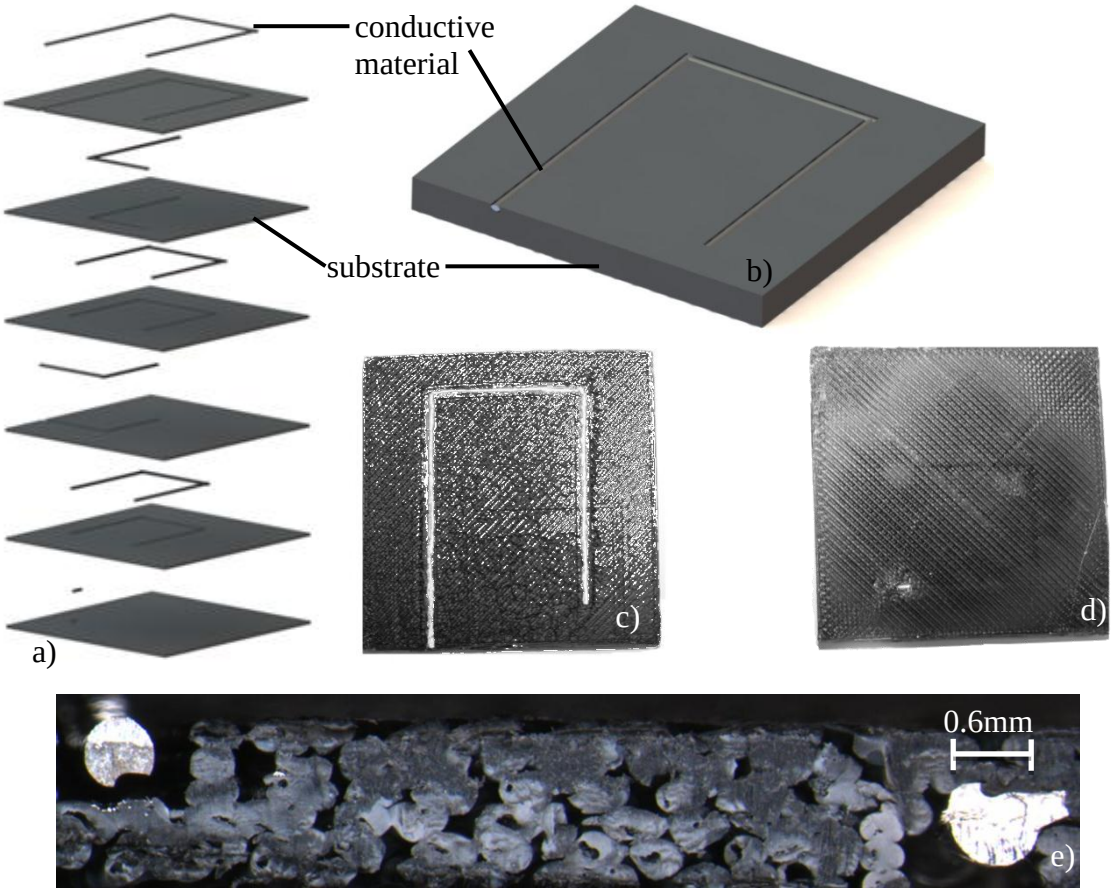

Figure 4 3D electronics using FDM where a) shows the stacking of ABS vias connecting each other with the Sn-Bi conductive material, b) showing the 3D model of the conductive material within the ABS substrate, c) is the top view of a built sample, d) is the bottom view of a built sample, and e) is the magnified view of a circuit cross-section at 72X showing the ABS layers with Sn-Bi within alternate layers.

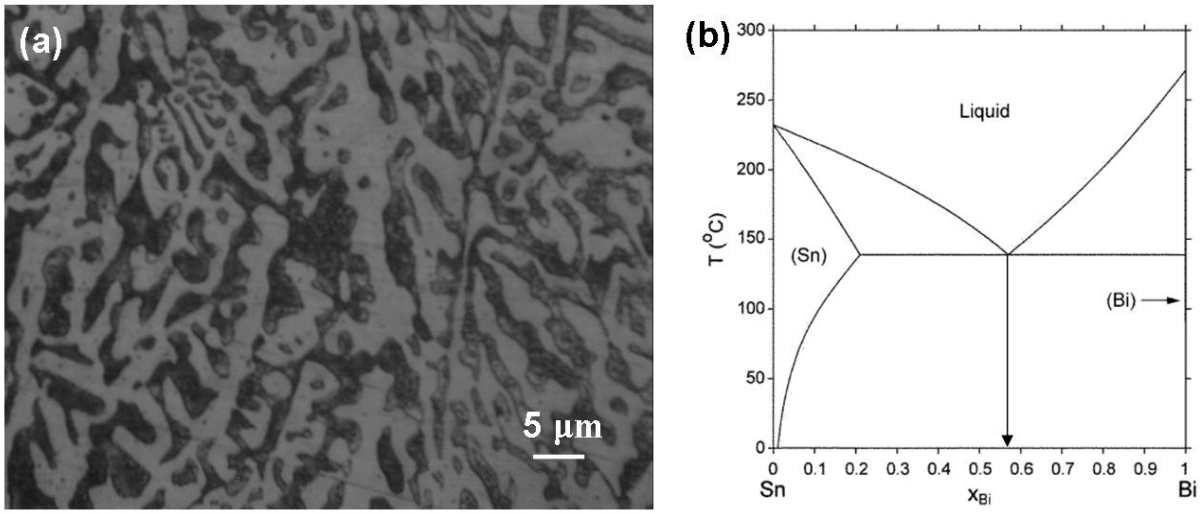

Figure 5: (a) Optical micrograph showing the eutectic microstructure and (b) corresponding phase diagram indicating the composition of our alloy (Kattner, 2002).

A potential application for FDMm is the building of 3D circuitry that allows for electrical components to be connected on different faces of a solid. Figure 4 demonstrates the ability for the support liquefier in the deposition head shown in Figure 1 to deposit a substrate and for the model liquefier to deposit the conductive material that connects to each layer through vias in the substrate material. Figures 4(a) and 4(b) show the CAD demonstration of the model while Figures 4(c) and 4(d) represent the actual deposition results. Figure 4(e) shows a magnified view taken with a stereomicroscope magnified at 72X of two subsequent layers showing Sn-Bi material filling the ABS via. Figure 4 only showed contacts between layers without electronic components; however, cavities which allow for component placement can be produced as demonstrated by Lopes *et al*. 2012 where stereolithography was used in the creation of 3D structural electronics.

4.3 Microstructural analysis

The optical metallograph (Figure 5) of the cross section of the FDM-built Bi58Sn42 solder component displays a two phase eutectic microstructure. This was consistent with what would be expected from the Sn-Bi phase diagram seen in Figure 5(b). Also observed in the cross

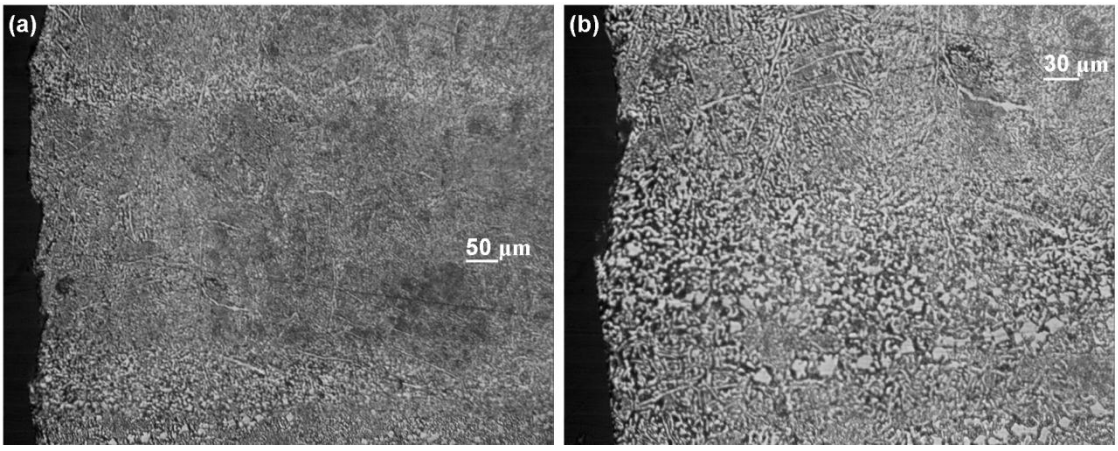

Figure 6: (a) The layering of fine and course microstructure observed on the cross-section of the FDM-Built component and (b) higher magnification image of the same area.

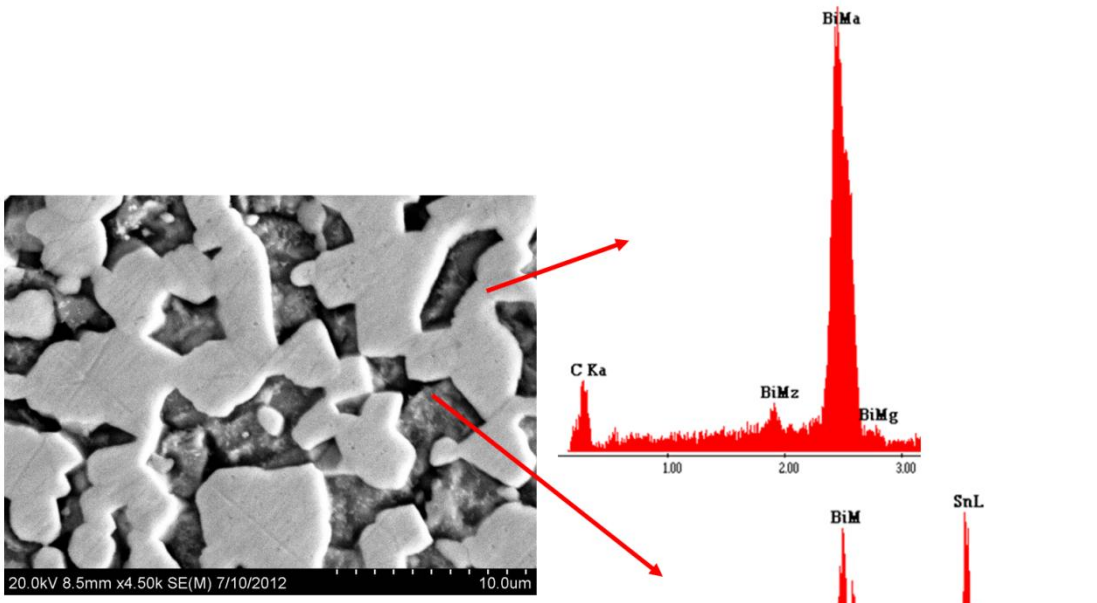

Figure 7: SEM micrograph and corresponding EDS spectra showing the differences between the two phases.

section (Figure 6) is a layering effect of fine and coarse microstructure which was most-likely due to the build process.

The SEM micrograph (Figure 7) of cross section of the FDM-built eutectic Bi58Sn42 solder component again showed a eutectic microstructure. Spot EDS analysis of the two phases reveals a Bi-rich phase with a Sn-Bi phase interdispersed throughout. Also observed within the microstructure was the same layering of fine and coarse lamella (Figure 8). The topography observed in Figure 8 was due to etch preparation as part of the metallographic process. The coarsening of the lamella may be due to the reheating of the previous build layer by the subsequent build

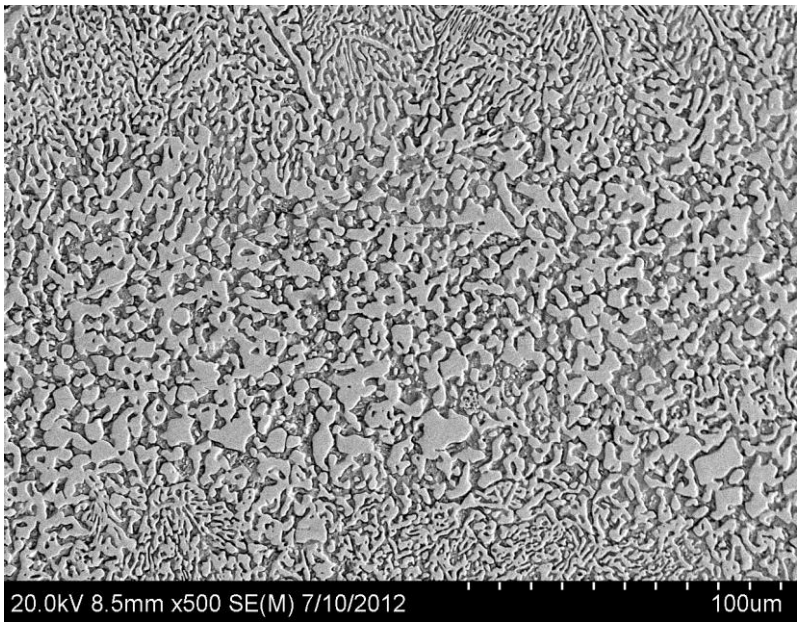

Figure 8: SEM micrograph showing the layering between fine and coarse microstructure

layer. In the context of a structural part, the coarsening of the eutectic microstructrure has been observed to improve the mechanical properties of Sn-Bi alloys used in various applications of low T_m alloys (Felton *et al*. 1993). In the context of the electric circuit presented here the coarsening may also be beneficial as, in general, a metallic conductive path with large grains will have better conductivity than the same material with small grains as grain boundaries act as detractors to the flow of electrons (Roberson, 2012).

Conclusions

Through the use of a FDM 3000 system, controlled deposition of metal alloys has been achieved and 3D structures have been built in a layered fashion using a redesigned liquefier. Idealistic modeling was done to evaluate the performance difference between the original liquefier and the redesigned liquefier. Assuming ideal conditions there were notable differences that exemplify the need for an improved liquefier design. Experimental measurements and deposition results further demonstrated the superior performance of the redesigned liquefier over the original liquefier. Various applications can benefit from metallic FDM including building jigs and fixtures, electroforming mandrels, encapsulation molds, dies, electronic joining applications, as well as printing 3-Dimensional circuitry. Microstructural analysis demonstrated good interlayer bonding with variations in the coarseness of microstructure along the layer interface that affects mechanical and conductive properties. The results of this work give potential to utilize the redesigned FDMm configuration with different deposition head materials to build metallic components using higher strength alloys.

Future Work

Further work can be extended to provide results using higher T_m metals which have potential applications in the fabrication of structural parts using the same methodology explored in this research. Accuracy has improved with the implementation of a redesigned deposition head; however, improvements are required to achieve accuracies equivalent to those achieved by polymers such as ABS (+-0.005). The fabrication of more complex 3D structures needs to be demonstrated and the microstructure and interfacial phenomena between layers for such structures needs to be analyzed. For 3D circuits, a fully-functional circuit needs to be demonstrated with cavities for electronic component placement. Control of microstructure may be accomplished by close control of temperature parameters to obtain favorable microstructures (coarsening) for maximum mechanical properties as well as uniform conductivity.

Acknowledgements

The research described in this paper was performed within the W.M. Keck Center for 3D Innovation at the University of Texas at El Paso (UTEP). Additional support was provided by the UTEP Louise Stokes Alliance for Minority Participation program funded through grant number HRD-1139929 from the National Science Foundation. The findings and opinions presented in this paper are those of the authors and do not necessarily reflect those of the sponsors of this research.

References

Agarwala, M. K., Weeren, R. V., Bandyopadhyay, A., Whalen, P. J., Safari, A., and Danforth, S. C., (1996), Fused Deposition of ceramics and metals: an overview. Proceedings of the Solid Freeform Fabrication Symposium, Austin, Texas.

Bellini A., and Bertoldi M., (2004). Liquefier dynamics in fused deposition modeling," Journal of Manufacturing Science and Engineering, 126, pp. 237-246.

Bellini A., (2002). Fused deposition of ceramics: A comprehensive experimental, analytical and computational study of material behavior, fabrication process and equipment design. Ph.D. Dissertation, Philadelphia, USA: Drexel University.

Chua, C.K., Leong, K.F., and Lim, C.S., (2003), Rapid prototyping: principles and applications, Singapore, World Scientific Publishing Co.

Felton, L., Raeder, C. & Knorr, D. (1993).The properties of tin-bismuth alloy solders. JOM Journal of the Minerals, Metals and Materials Society 45, 28–32.

Finke, S., Feenstra, F.K., (2002). Solid Freeform fabrication by extrusion and deposition of semi-solid alloys. Journal of Materials Science, 37, pp. 3101-3106.

Kattner, U.R., (2002). Phase diagrams for lead-free solder alloys. Journal of Materials. 54 (45). pp.45-50.

Lopes, A.J., MacDonald, E., Wicker, R., (2012). Integrating stereolithography and direct print technologies for 3D structural electronics fabrication. Rapid Prototyping Journal, 18 (2), pp.129-143.

Masood, S., and Song, W.Q., (2004). Development of new metal/polymer materials for rapid tooling using fused deposition modeling. Materials & Design, **25**(7), pp. 587-594.

Mireles, J., Kim, H., Lee, I.H., Espalin, D., Medina, F., MacDonald, E., Wicker, R., (2012). Development of a Fused Deposition Modeling system for low temperature metal alloys. Journal of Electronic Packaging.

Ojebuoboh, F.K., (1992). Bismuth-Production, properties, and applications. Journal of Materials: 1992 Review of Extractive Metallurgy, 44 (4), pp.46-49.

Ramanath, H.S., Chua, C.K., Leong, K.F., Shah, K.D.,(2008). Melt flow behavior of poly-ε-caprolactone in fused deposition modeling. Journal of Materials Science, 19 (7), pp. 2541-2550.

Roxas, M., Ju, S., (2008). Fluid dynamics analysis of desktop-based fused deposition modeling rapid prototyping. Department of Mechanical and Industrial Engineering, University of Toronto.

Rice, C.S., Mendez, P.F., Brown, S.B., (2000). Metal solid freeform fabrication using semi-solid slurries. Journal of Minerals, Metals, and Materials Society, 52 (12), pp. 31-33.

Roberson, D. A. Dissertation, The University of Texas at El Paso, (2012)

White, C.E.T., Ferriter, J.M., (1990). How to use fusible alloys. Machine Design, 62 (25), pp. 124-131.